Geospatial Analysis for Erosion and Sediment Yield Estimation: The Case Study of the Krueng Aceh River Basin, Indonesia

Miga Magenika Julian
Hydrography Research Group, Faculty of Earth Science and Technology, Institut Teknologi Bandung, Indonesia
miga.m.julian@itb.ac.id

Esa Fajar Hidayat
Marine Science Study Program, Faculty of Fisheries and Marine Science, Universitas Brawijaya, Indonesia
esafajarh21@ub.ac.id (corresponding author)

Nirmawana Simarmata
Geomatics Engineering Department, Institut Teknologi Sumatera, Indonesia
nirmawana.simarmata@gt.itera.ac.id

Received: 9 March 2026 | Revised: 22 April 2026 | Accepted: 30 April 2026

 DOI: https://doi.org/10.48084/etasr.18606

ABSTRACT

The Krueng Aceh River Basin (KARB) has undergone severe environmental degradation due to deforestation, land use changes, and the 2004 tsunami, resulting in increased erosion and sedimentation. This study estimated sediment yield using the Revised Universal Soil Loss Equation (RUSLE) and Sediment Delivery Ratio (SDR) models integrated with Geographic Information System (GIS) across five sub-basins covering 1,734 km². Input data included DEM, soil type, land use, and rainfall. Erosion rates ranged from 0 to 1.4×10^{7} tons/km²/year, with higher values observed in steep slopes, bare land, and erosion-prone soils, particularly in the Krueng Jreue and Krueng Inong sub-basins. SDR analysis showed greater transport efficiency for silt (2.8×10^{-2}) than sand (2.7×10^{-3}). The estimated total sediment yield was 2.4×10^{6} tons/year. Land use analysis highlighted that bare land (19% of the area) contributed significantly to erosion, while forest cover (29%) provided limited mitigation. The study underscores the urgency of integrated watershed management and reforestation efforts in KARB.

Keywords-erosion; GIS; river basin; sediment delivery ratio; watershed management

I. INTRODUCTION

The environmental condition of the Krueng Aceh River Basin (KARB) has declined. Forest damage in the upstream of the river basin may result in increased water and sediment discharge [1, 2], decreasing the river basin's resilience to rainwater and runoff. The high intensity of rain and the speed of water flow lead to erosion and sedimentation [3]. Moreover, the tsunami that struck Aceh in 2004 caused damage along the coastal area [4]. One of the affected areas is the river outlet of the KARB. Sediments exported from the river basin to the coastal area serve to maintain the stability of the coastal environment. By managing the total sediment exported from the KARB, the condition of the coastal area at the outlet will improve. Therefore, information on the erosion potential and the total sediment exports is essential for managing a river basin environment [5].

Soil erosion is one of the most common environmental problems in watersheds, especially in high-rainfall areas such as Aceh. Erosion can cause the loss of fertile soil layers, reducing the overall soil fertility, as well as land degradation. In addition, erosion contributes to sedimentation in water bodies, reducing the storage capacity of rivers and reservoirs and disrupting aquatic ecosystems. In the Krueng Aceh watershed, increased human activities such as land clearing for agriculture, infrastructure development, and land use change have accelerated erosion and sedimentation processes [6]. Modeling erosion and sedimentation using Geographic Information System (GIS) technology has become increasingly important in environmental studies and natural resource management. GIS enables efficient collection, processing, and analysis of geospatial data and provides better insights into the spatial and temporal distribution of erosion and sedimentation processes [7].

This study will estimate the total sediment exported by the KARB using the erosion and sediment delivery models. GIS is implemented in spatial modeling, as other researchers have done for river basin ecosystems [8, 9]. Sediment yield is calculated, including the erosion rate and Sediment Delivery Ratio (SDR). Additionally, sediment particle sizes are characterized, with silt (10 µm) representing fine sediment and sand (100 µm) representing coarse sediment. The spatial distribution of sediment yield allows for investigating the criticality of the KARB over the erosion processes. Finally, the results of this study are expected to act as a scientific reference to develop better adaptation strategies that account for land cover impacts and river basin management.

II. MATERIALS AND METHODS

A. Study Area

The study area includes the KARB, which has five sub-basins, namely the Krueng Aceh Hilir, Krueng Jreue, Krueng Keumireu, Krueng Inong, and Seulimum Sub-Basin, as shown in Figure 1. The KARB is located between 95°01'00"E and 95°50'00"E longitude and 5°01'00"N and 5°40'00"N latitude. The total area of the KARB is 1,734 km² with an average slope of 9 degrees. Agricultural areas dominate land use, with 49% of the total basin area. The dominant soil type is latosol. The average rainfall is about 1,700 mm per year.

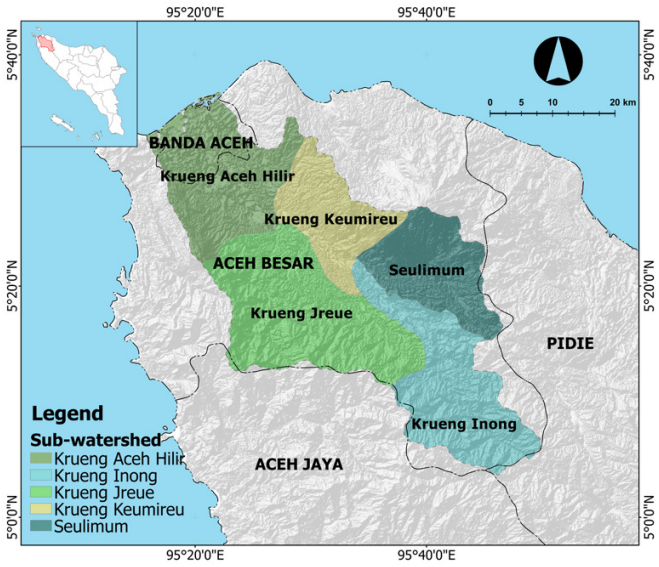

Fig. 1. The KARB study area.

B. Data

The geospatial data utilized in this study include Digital Elevation Model (DEM), Land Use and Land Cover (LULC) classifications, soil type distributions, and precipitation records. These specific parameters were selected due to their crucial role in driving and characterizing the erosion and sedimentation processes within the KARB.

1) Digital Elevation Model

DEM was acquired from the Shuttle Radar Topography Mission (SRTM) [10]. SRTM data were produced by the National Aeronautics and Space Administration (NASA). SRTM has a spatial resolution of 90 m and 16 m of vertical precision at a 90% confidence level. SRTM DEM can be generated for the slope, drainage network, and flow length parameters. DEM data are essential for calculating slope steepness, flow direction, and flow accumulation, directly affecting erosion rates and sediment transport.

2) Land Use and Land Cover

LULC data were obtained from Landsat TM 2005 satellite imagery with a spatial resolution of 30 m and classified using a supervised approach. The classification categories include forest, agricultural land, bare land, urban areas, and water bodies. These LULC types influence erosion by affecting vegetation cover, surface runoff, and soil stability. For example, bare land and agricultural land with minimal cover exhibit higher erosion rates than forested areas, which act as natural erosion barriers.

3) Soil Types

Soil-type data were sourced from the Harmonized World Soil Database (HWSD), including parameters such as texture, organic matter content, and erodibility factor (K factor). These characteristics are crucial for estimating soil erosion potential. Sandy soils in the study area were found to have lower water retention capacity and higher susceptibility to erosion, whereas clay-rich soils exhibited more cohesive properties, reducing erosion risk.

4) Rainfall

Rainfall data were obtained from Climate Hazards InfraRed Precipitation with Station (CHIRPS) data. The rainfall data include monthly and annual precipitation averages, which are used to calculate the rainfall erosivity factor (R) in the Revised Universal Soil Loss Equation (RUSLE). High-intensity rainfall events significantly contribute to surface runoff and sediment transport, especially in areas with poor vegetation cover. CHIRPS data have a spatial resolution of 0.05° (~5.3 km at the equator), ensuring adequate spatial coverage for the study area.

C. Estimation of Sediment Yield from a River Basin

The erosion process model was built to estimate the total sediment yield (Y) by a river basin system, as displayed in Figure 2. SDR states the ratio of sediment exported from the river basin system (Y) to the eroded sediment from its source (E):

$$\text{SDR} = \frac{Y}{E} \quad (1)$$

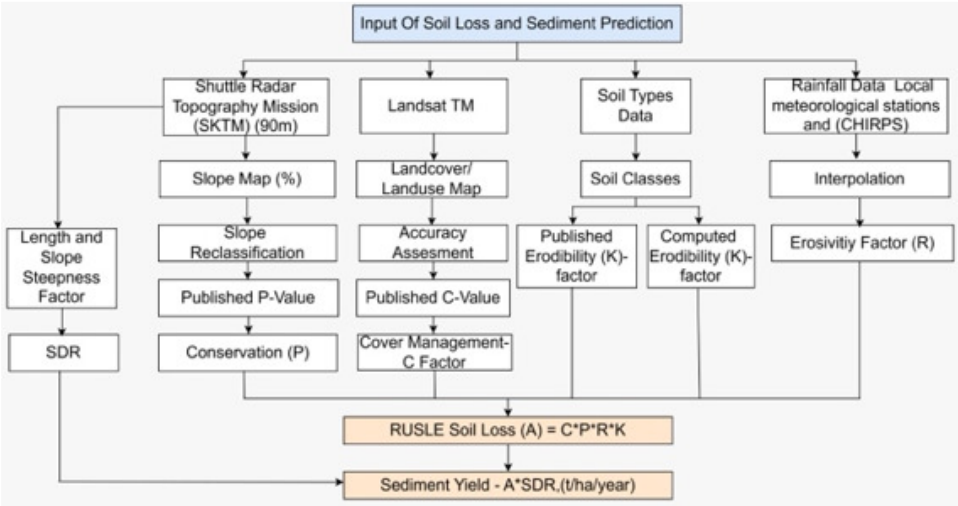

Fig. 2. Flow chart of sediment yield estimation.

SDR is estimated based on the physical process of sediment transport at the hillslopes and drainage networks of the river basin [11]. The efficiency of transporting eroded sediments is influenced by the sediment transport medium's travel time, namely, water flow. Water travel time is calculated by:

$$t = \frac{D}{V} \quad (2)$$

where D is the flow distance, and V is the flow speed. D is generated from DEM. V is influenced by the slope, rainfall intensity, and surface roughness coefficient. V is calculated at the hillslopes and drainage networks of the river basin.

On the hillslopes, V is calculated using [12]:

$$V = \frac{\left(i_e L\right)^{0.4} s^{0.3}}{n^{0.6}} \quad (3)$$

where i_e is the excess rainfall, L is the distance of the river flow, s is the slope, and n is the Manning surface roughness coefficient.

In drainage networks, V is calculated using [13]:

$$V = as^{0.5} \quad (4)$$

where s is the slope, and a is the river roughness coefficient.

Manning's roughness coefficient (n) and riverbed roughness coefficient are illustrated in Tables I and II, respectively [11].

TABLE I. MANNING'S ROUGHNESS COEFFICIENT (N) [11]

Land use type	C_v (%)		
	C_v<30	30<C_v<70	C_v>30
Grassland, shrub, pastures	0.15	0.4	0.6
Crop land	0.15	0.25	0.4
Forest	0.2	0.6	0.8
Built-up areas	0.1	0.3	0.5
Wet land, ponds, rivers	0.125	0.125	0.125

TABLE II. RIVERBED ROUGHNESS COEFFICIENT [11]

River section	Upstream area (Ha)	a
Concentrated shallow flow	1.8–18	4
Intermitten stream	18–360	4.5
Permanent stream	>360	5

SDR is affected by sediment residence time, which states the duration of time it takes for sediment to stay in a river basin system, and it is proportional to the travel time of the flow. Sediment residence times are calculated on the hillslopes and drainage networks of the river basin using:

$$t_h = t_{hw} e^{(\gamma_h w_s)} \quad (5)$$

$$t_n = t_{nw} e^{(\gamma_n w_s)} \quad (6)$$

where t_{hw} is the travel time on the hillslopes, t_{nw} is the travel time on the drainage network, γ_h and γ_n are factors that are inversely proportional to the flow of water, γ_h is h_h-1, and γ_n is h_n-1, with h_h being the depth of the hillslope flow, h_n is the depth of the drainage network flow, and w_s is the sediment fall speed. In this study, the depth of hillslope flow is set at 1 cm and the depth of drainage network flow at 1 m.

Finally, the efficiency of SDR is estimated using:

$$\text{SDR} = \frac{t_n}{t_n - t_h}\left\{1 - \exp\left(-\frac{t_{er}}{t_n}\right)\right\} - \frac{t_h}{t_n - t_h}\left\{1 - \exp\left(-\frac{t_{er}}{t_h}\right)\right\} \quad (7)$$

where t_{er} is the duration of effective rainfall, which is a function of the average rainfall.

Soil particles that have been eroded from their sources are calculated by the empirical model of the RUSLE, using [14]:

$$E = L_S C K R P \quad (8)$$

where E is the erosion rate, L_S is the slope index, C is the land-use factor, K is the soil erodibility, and R is the rainfall erosivity.

C factor is a value that states the effect of land-use on erosion, as depicted in Table III [17]. The effect of land-use on erosion is to protect the soil surface from rainwater collisions by decreasing the speed and diameter of rainwater, while also decreasing the speed and volume of water flow. Erosivity (*R*) is a value that indicates the amount of external force that comes from rainfall to release sediment particles from the soil surface. Erodibility (*K*) is a value that indicates whether sediment particles are easily detached from the soil by surface runoff, as exhibited in Table IV [18]. The dominant soil properties in determining erodibility are soil texture and infiltration capacity [15].

Slope index (L_S) is obtained from the DEM in the study area using [11]:

$$L_s = (\frac{L}{K})^m (k_1 \, sin^2 \, s + \, k_2 \sin s + \, k_3) \quad (9)$$

where *L* is the flow length on the surface of DEM with a value greater than 122m [16], *m* is the slope category, *s* is the slope percentage, and *k* are empirical constants. The slope category is $m = 0.2$ for $0 \leq s < 1$, $m = 0.3$ for $1 \leq s < 3$, m = 0.4 for $3 \leq s < 4.5$, and $m = 0.5$ for $s \geq 4.5$, whereas the empirical constants are $k = 22.1$, $k_1 = 65.41$, $k_2 = 4.56$, and $k_3 = 0.065$.

Erosivity (*R*) is expressed as a function of rainfall [14] using:

$$R = 2.21P^{1.36} \quad (10)$$

where *P* is the monthly rainfall in cm.

The *P* factor is set at 1.0. This is because systematic conservation practices, such as widespread terracing or specific structural erosion controls, are not uniformly applied or documented across the KARB.

TABLE III. LAND USE VALUE [17]

Land use	*C* factor
Rivers, ponds, lakes	0.0001
Industrial zone	0.0005
Residential	0.0007
Aquatic vegetation, wetland	0.001
Forest	0.002
Shurb, pastures, park	0.003
Farm, dry field	0.005
Bare land	0.4
Mining zone	0.7

TABLE IV. ERODIBILITY VALUE [18]

Soil type	Erodibility (K)	Code
Alluvial, planosol, gray hydromorf, lateric, gley	0.20	3
Latosol	0.23	1
Mediteran	0.24	2
Andosol, grumosol, podsol, podsolic	0.26	0
Regosol, litosol, organosol, renzina	0.31	2

III. RESULTS AND DISCUSSION

The results of the estimated erosion rate (*E*) in the KARB ranged from 0-1.4×107 tons/km²/year, with an average of 1.2×105 tons/km²/year. High magnitude of *E* was mainly located in areas with steep topography, bare land area, and very erosion-sensitive soil types, namely regosols, as demonstrated in Figure 3. Such areas are concentrated in the Krueng Inong sub-basin with an average *E* of 2.4×105 tons/km²/year, and in the Krueng Jreue sub-basin with an average *E* of 1.7×105 tons/km²/year. High *E* indicates that many soil particles are detached from the surface of the soil. Low *E* was produced in the downstream of the KARB with gently sloping topography.

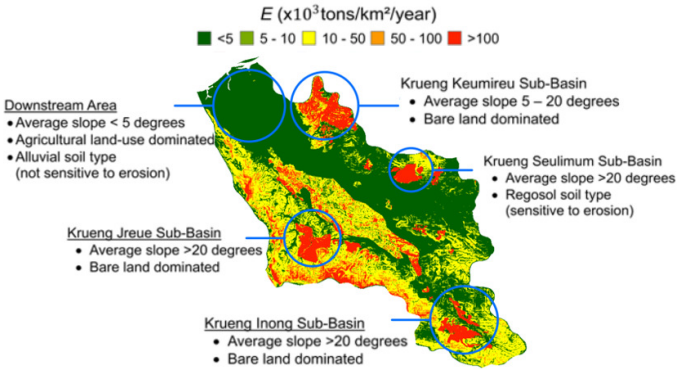

Fig. 3. Spatial distribution of erosion rates.

SDR values were calculated for two types of sediment particles, namely silt particles with a diameter of 10 µm and sand with a diameter of 100 µm. The falling speed of the two sediment particles was 9×10^{-6} m/s and 7×10^{-3} m/s, respectively. The SDR value is inversely proportional to the high *E,* which means that SDR is strongly related to low *E* generated in the lower KARB. The SDR value is concentrated in areas with sloping topography; that is, along the middle of the KARB, as illustrated in Figure 4. SDR indicates efficiency for transporting eroded sediment. A higher SDR magnitude indicates greater sediment transport. SDR magnitude is inversely proportional to the diameter of sediment particles. The smaller the diameter of a particle, the easier it will be transported by water flow. Overall SDR values were at intervals of 8.38×10^{-5}-0.66 with an average of 2.8×10^{-2} for silt particles, and 2.86×10^{-6}-0.25 with an average of 2.7×10^{-3} for sand particles.

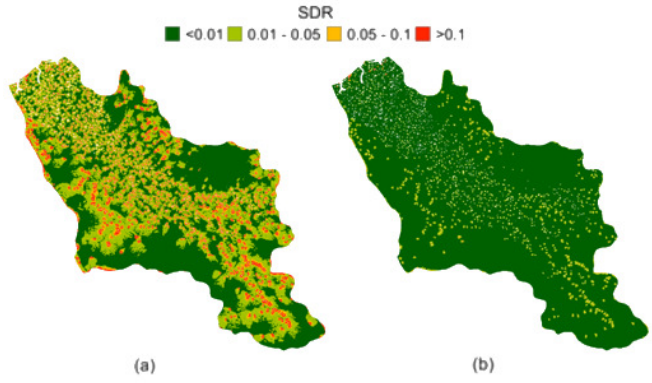

Fig. 4. Spatial Distribution of SDR: (a) silt and (b) sand.

The distribution of the results of the modelling of sediment export rate (Y) is shown in Figure 5. Y values for silt that reached 10,000 tons/km²/year were concentrated in the Krueng Jreue sub-basin and the Krueng Inong sub-basin. For sand, the highest Y was produced in Krueng Jreue, Krueng Keumireu, and Krueng Inong sub-basins at intervals of 100-1,000 tons/km²/year. The results of silt and sand sediments were concentrated in the same area but with different intensities.

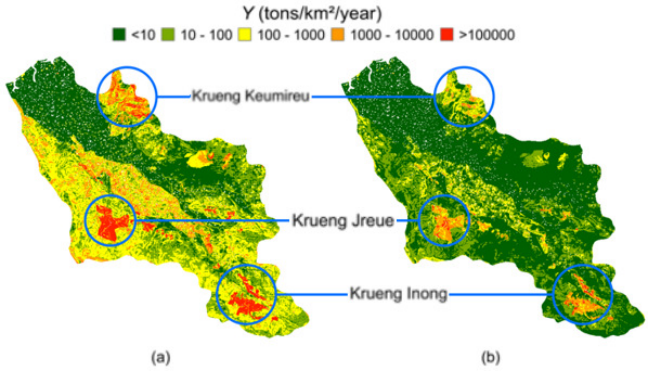

Fig. 5. Spatial distribution of sediment yield (Y): (a) silt and (b) sand.

The distribution of sediment yield is proportional to the increase in erosion rate. Comparing Figures 3 and 5, it can be seen that areas with high Y values are areas with high erosion potential. The high Y value was produced in areas with steep topography and land use conditions in the form of bare land areas. Areas with these characteristics are often found in the Krueng Jreue and Krueng Inong sub-basins. The model results for each sub-basin are outlined in Table V. Total sediment released from the river basin system (Y_{tot}) is assumed to be composed of silt and sand sediment particles. The uniformity was assumed due to the unavailability of sediment size distribution data in the study area. Y_{tot} obtained from the calculation results in the KARB was 2.4 × 106 tons/year.

Previous studies agree that sub-basins with land-use conditions in the form of bare land produce high erosion rates [19]. The condition of land-use that is not protected by vegetation will increase the generating force of rainfall when it hits the ground surface. The bare land area of the KARB is 19% of the total river basin area, as seen in Figure 6. The most dominant land-use is the agricultural area, with an area of 844 km² or about half of the basin area. Forest cover is only about one-third of the total basin area. Turning forests into agricultural and bare land areas is a cause of high erosion potential in a river basin [20, 21].

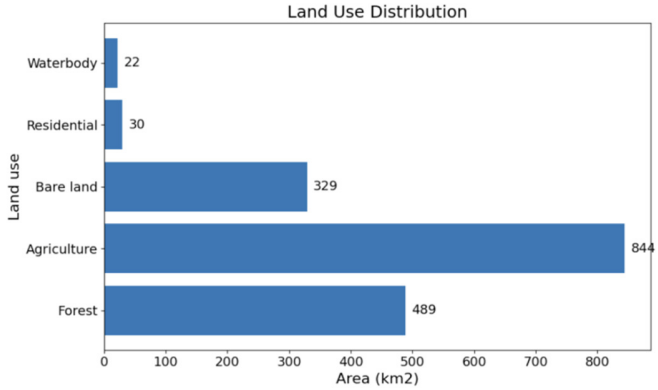

Fig. 6. Percentage area of land-use in the KARB.

According to the results of accuracy tests using reference data from the National Geospatial Information Agency, the Overall Accuracy (OA) was 85%, and the Kappa coefficient was 83.12%, indicating a high level of accuracy with very strong agreement. This high accuracy is influenced by the dominance of major classes such as agriculture and forest, which have more stable spectral characteristics, although potential errors may still occur in classes with spectral similarities, such as open land and settlements. Overall, these classification results can be considered reliable and suitable for use as a basis for further geospatial analysis at the watershed scale.

Based on sediment export rates, the level of potential erosion is classified as normal erosion, critical erosion, and supercritical erosion [22]. The distribution of erosion rate levels in the KARB is presented in Figure 7. Normal erosion produces a sediment export rate of 0-3,000 tons/km²/year. Sediment export rates between 3,000 and 10,000 tons/km²/year are produced in areas with critical erosion. Areas with supercritical erosion produce sediment export rates of more than 10,000 tons/km²/year. In general, the level of erosion in the KARB is still classified as normal erosion. Supercritical erosion is concentrated in the Krueng Jreue sub-basin, Inong, and a small part of the Krueng Keumireu sub-basin.

TABLE V. E, SDR, Y, AND Y_{TOT} PER SUB-BASIN

Sub-Basin	Area (km²)	E (tons/km²/year)	SDR		Y (tons/km²/year)		Y_{tot} (tons/year)	
			Silt	Sand	Silt	Sand	Silt	Sand
Krueng Aceh Hilir	352	2.6×10^4	0.0173	0.0016	455	42	1.5×10^5	1.4×10^4
Krueng Inong	279	2.4×10^5	0.0268	0.0024	6564	598	1.8×10^6	1.6×10^5
Krueng Jreue	519	1.6×10^5	0.0218	0.0018	3607	307	1.9×10^6	1.5×10^5
Krueng Keumireu	243	7.4×10^4	0.0181	0.0016	1353	127	3.2×10^5	3×10^4
Seulimum	341	6.9×10^4	0.0086	0.0007	598	49	2×10^6	1.6×10^4
Average in KARB		1.14×10^5	0.01852	0.00162	2515.4	224.6	1.23×10^6	7.4×10^4

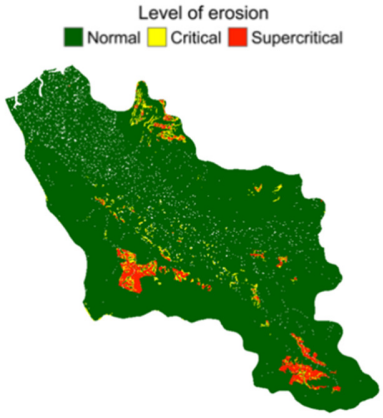

Fig. 7. Level of potential erosion.

Due to the unavailability of observed sediment yield data in the KARB, a comparative assessment was carried out by benchmarking the modeled sediment export against the Upper Citarum River Basin, Indonesia [10], a watershed whose sediment export data have been previously validated using observed field data. The two basins share comparable spatial extents, namely 1,734 km² for the KARB and 1,771 km² for the Upper Citarum. Furthermore, the topography of both river basins is broadly similar, with an average slope of 9° for the KARB and 8° for the Upper Citarum. As shown in Table VI, these similarities in basin size, slope, and the relative proportion of forest cover result in modeled sediment yields of a similar order of magnitude, providing a useful baseline reference for the KARB estimates.

TABLE VI. EROSION MODELING RESULTS FOR THE KRUENG ACEH AND UPPER CITARUM RIVER BASIN

Comparison factor	**KARB**	**Upper Citarum River Basin**	**Percentage of deviation**
Area of river basin (km^2)	1734	1771	-2%
Average slope (°)	9	8	13%
Area of forest cover (%)	29	21	38%
Y_{tot} ($\times 10^6$ tons/years)	2.4	2.1	14%

While this study provides a comprehensive geospatial assessment of erosion and sediment yield in the KARB, a major limitation must be acknowledged regarding model validation. Due to the unavailability of observed, in-situ sediment yield data within the KARB, direct empirical validation of the model sediment export rates was not currently possible. However, the application of combined RUSLE and SDR frameworks remains a widely accepted and robust methodology for establishing baseline sediment yield estimates and identifying high-priority sub-watersheds in ungauged or data-scarce river basins [23]. To establish a level of confidence in the model's outputs, this study employed a comparative approach against the Upper Citarum River Basin, which shares similar topographic slopes and forest cover percentages and has been previously validated. This comparison serves as a relative benchmark rather than proper local validation. Sediment yield dynamics are highly sensitive to spatial heterogeneity and basin-specific characteristics, including underlying lithology, localized rainfall intensity, drainage density, and specific sediment connectivity pathways [24, 25]. These variables dictate the nonlinear nature of sediment detachment and transport, inherently differing between the Krueng Aceh and Citarum basins. Consequently, the estimated total sediment yield of 2.4×10^6 tons/year represents a modeled magnitude of potential sediment export rather than an absolute measured value. These uncertainties underscore that while GIS-based modeling is an essential predictive tool for identifying critically degraded sub-basins, absolute values carry inherent margins of error. This highlights the necessity for future research to establish long-term hydrometric and sediment monitoring stations at the KARB outlet to properly calibrate and validate these predictive models.

IV. CONCLUSIONS

This study assessed erosion and sediment export in the Krueng Aceh River Basin (KARB) using Geographic Information System (GIS)-based modeling. The results indicated that areas with steep topography and bare land, such as the Krueng Inong and Krueng Jreue sub-basins, experience the highest erosion rates and sediment yields. Silt particles were more efficiently transported than sand, underscoring particle size's significance in sediment dynamics. The total sediment yield exported from the KARB was estimated at 2.4×10^6 tons/year, with critical contributions from sub-basins where vegetation cover is limited, and soil types are prone to erosion. The findings highlight the need for integrated watershed management strategies. Efforts should focus on reforestation, sustainable land use practices, and soil conservation measures to mitigate erosion and sedimentation in the KARB. Agricultural activities should adopt contour farming, terracing, and agroforestry practices to minimize soil loss.

Further research is needed to investigate sediment composition and its impact on aquatic ecosystems. Studies that integrate socioeconomic data with biophysical models can provide a more holistic understanding of human-environment interactions, allowing for tailored management interventions that align with community needs. Additionally, future research should also focus on policy recommendations for sustainable watershed management, informed by scientific findings, to facilitate effective land-use regulations and conservation initiatives.

DECLARATION OF COMPETING INTERESTS

The authors declare no competing interests.

ACKNOWLEDGMENT

This research received no specific grant from any funding agency in the public, commercial, or not-for-profit sectors.

DATA AVAILABILITY

All data that support the findings of this study are included within the article.

REFERENCES

[1] L. A. Bruijnzeel, "Hydrological functions of tropical forests: not seeing the soil for the trees?," *Agriculture, Ecosystems & Environment*, vol. 104, no. 1, pp. 185–228, Sept. 2004, https://doi.org/10.1016/j.agee.2004.01.015.

[2] T. Ferijal, Mustafril, D. S. Jayanti, and Dahlan, "Modeling Hydrologic Response to Land Use and Climate Change in the Krueng Jreu Sub Watershed of Aceh Besar," *Aceh International Journal of Science and Technology*, vol. 5, no. 3, pp. 116–125, Dec. 2016, https://doi.org/10.13170/aijst.5.3.5762.

[3] J. Vermang, L. d. Norton, C. Huang, W. m. Cornelis, A. m. da Silva, and D. Gabriels, "Characterization of Soil Surface Roughness Effects on Runoff and Soil Erosion Rates under Simulated Rainfall," *Soil Science Society of America Journal*, vol. 79, no. 3, pp. 903–916, July 2015, https://doi.org/10.2136/sssaj2014.08.0329.

[4] R. Cochard, S. L. Ranamukhaarachchi, G. P. Shivakoti, O. V. Shipin, P. J. Edwards, and K. T. Seeland, "The 2004 tsunami in Aceh and Southern Thailand: A review on coastal ecosystems, wave hazards and vulnerability," *Perspectives in Plant Ecology, Evolution and Systematics*, vol. 10, no. 1, pp. 3–40, Mar. 2008, https://doi.org/10.1016/j.ppees.2007.11.001.

[5] R. C. Sidle *et al.*, "Sediment Sources, Erosion Processes, and Interactions with Climate Dynamics in the Vakhsh River Basin, Tajikistan," *Water*, vol. 16, no. 1, 2024, Art. no. 122, https://doi.org/10.3390/w16010122.

[6] S. Sugianto, A. Deli, E. Miswar, M. Rusdi, and M. Irham, "The Effect of Land Use and Land Cover Changes on Flood Occurrence in Teunom Watershed, Aceh Jaya," *Land*, vol. 11, no. 8, Aug. 2022, Art. no. 1271, https://doi.org/10.3390/land11081271.

[7] P. Naveen, R. Maheswar, and P. Trojovský, "GeoNLU: Bridging the gap between natural language and spatial data infrastructures," *Alexandria Engineering Journal*, vol. 87, pp. 126–147, Jan. 2024, https://doi.org/10.1016/j.aej.2023.12.027.

[8] M. M. Julian, A. Brenning, S. Kralisch, and M. Fink, "Modelling of Hydrological Responses in the Upper Citarum Basin based on the Spatial Plan of West Java Province 2029 and Climate Change," *International Journal of Technology*, vol. 10, no. 5, pp. 866–875, Oct. 2019, https://doi.org/10.14716/ijtech.v10i5.2376.

[9] Poerbandono, A. B. Harto, and M. M. Julian, "Spatial Decision Assistance of Watershed Sedimentation (SDAS): Development and Application," *Journal of Engineering and Technological Sciences*, vol. 46, no. 1, pp. 37–57, Apr. 2014, https://doi.org/10.5614/j.eng.technol.sci.2014.46.1.3.

[10] NASA JPL, "NASA Shuttle Radar Topography Mission Global 1 arc second number." NASA Land Processes Distributed Active Archive Center, 2013.

[11] H. Lu, C. J. Moran, and I. P. Prosser, "Modelling sediment delivery ratio over the Murray Darling Basin," *Environmental Modelling & Software*, vol. 21, no. 9, pp. 1297–1308, Sept. 2006, https://doi.org/10.1016/j.envsoft.2005.04.021.

[12] D. E. Overton and M. E. Meadows, *Stormwater modeling*. New York: Academic Press, 1976.

[13] C. T. Haan, B. J. Bartfield, and J. C. Hays, *Design Hydrology and Sedimentology for Small Catchments*. New York: Academic Press, 1994.

[14] W. H. Wischeimer and D. D. Smith, *Predicting Rainfall Erosion Losses: A Guide to Conservation Planning*. Hyattsville, MD: United States Department of Agriculture, 1978.

[15] C. Asdak, *Hidrologi dan Pengelolaan Daerah Aliran Sungai*. Yogyakarta: Gadjah Mada University Press, 1995.

[16] K. G. Renard, G. R. Foster, G. A. Weesies, D. K. McCool, and D. C. Yoder, *Predicting Soil Erosion by Water: A Guide to Conservation Planning with the Revised Universal Soil Loss Equation (RUSLE)*. Washington DC: United States Department of Agriculture, 1997.

[17] N. Trahan, Modeling sediment and contaminant pathways to the Cedar River. Florida: Jones, Edmunds & Associates, 2003.

[18] A. G. Kartasapoetra, *Teknologi Konservasi Tanah dan Air*, 6th ed. Jakarta: Rineka Cipta, 2010.

[19] C. Fernandez, J. Q. Wu, D. K. McCool, and C. O. Stockle, "Estimating water erosion and sediment yield with GIS, RUSLE, and SEDD," *Journal of Soil and Water Conservation*, vol. 58, no. 3, pp. 128–136, 2003.

[20] N. Nut *et al.*, "Land Use and Land Cover Changes and Its Impact on Soil Erosion in Stung Sangkae Catchment of Cambodia," *Sustainability*, vol. 13, no. 16, Aug. 2021, Art. no. 9276, https://doi.org/10.3390/su13169276.

[21] Poerbandono, A. Basyar, and A. B. Harto, "Spatial Modeling of Sediment Transport over the Upper Citarum Catchment," vol. 38, no. 1, pp. 11–28, 2006.

[22] H. R. Mulyanto, *Sungai: fungsi dan sifat-sifatnya*. Semarang: Graha Ilmu, 2006.

[23] S. Swarnkar, A. Malini, S. Tripathi, and R. Sinha, "Assessment of uncertainties in soil erosion and sediment yield estimates at ungauged basins: an application to the Garra River basin, India," *Hydrology and Earth System Sciences*, vol. 22, no. 4, pp. 2471–2485, Apr. 2018, https://doi.org/10.5194/hess-22-2471-2018.

[24] T. M. Massong and D. R. Montgomery, "Influence of sediment supply, lithology, and wood debris on the distribution of bedrock and alluvial channels," *GSA Bulletin*, vol. 112, no. 4, pp. 591–599, Apr. 2000, https://doi.org/10.1130/0016-7606(2000)112%253C591:IOSSLA%253E2.0.CO;2.

[25] E. R. Mueller and J. Pitlick, "Sediment supply and channel morphology in mountain river systems: 1. Relative importance of lithology, topography, and climate," *Journal of Geophysical Research: Earth Surface*, vol. 118, no. 4, pp. 2325–2342, 2013, https://doi.org/10.1002/2013JF002843.